

Research Article

Genome mining of astaxanthin biosynthetic genes from *Sphingomonas* sp. ATCC 55669 for heterologous overproduction in *Escherichia coli*

Tian Ma¹, Yuanjie Zhou¹, Xiaowei Li¹, Fayin Zhu¹, Yongbo Cheng¹, Yi Liu¹, Zixin Deng¹ and Tiangang Liu^{1,2,3}

¹ Key Laboratory of Combinatorial Biosynthesis and Drug Discovery (Wuhan University), Ministry of Education, Wuhan University School of Pharmaceutical Sciences, Wuhan, PR China

² Hubei Engineering Laboratory for Synthetic Microbiology, Wuhan Institute of Biotechnology, Wuhan, PR China

³ Hubei Provincial Cooperative Innovation Center of Industrial Fermentation, Wuhan, PR China

As a highly valued keto-carotenoid, astaxanthin is widely used in nutritional supplements and pharmaceuticals. Therefore, the demand for biosynthetic astaxanthin and improved efficiency of astaxanthin biosynthesis has driven the investigation of metabolic engineering of native astaxanthin producers and heterologous hosts. However, microbial resources for astaxanthin are limited. In this study, we found that the α -Proteobacterium *Sphingomonas* sp. ATCC 55669 could produce astaxanthin naturally. We used whole-genome sequencing to identify the astaxanthin biosynthetic pathway using a combined PacBio-Illumina approach. The putative astaxanthin biosynthetic pathway in *Sphingomonas* sp. ATCC 55669 was predicted. For further confirmation, a high-efficiency targeted engineering carotenoid synthesis platform was constructed in *E. coli* for identifying the functional roles of candidate genes. All genes involved in astaxanthin biosynthesis showed discrete distributions on the chromosome. Moreover, the overexpression of exogenous *E. coli* *idi* gene in *Sphingomonas* sp. ATCC 55669 increased astaxanthin production by 5.4-fold. This study described a new astaxanthin producer and provided more biosynthesis components for bioengineering of astaxanthin in the future.

Received	29 APR 2015
Revised	07 AUG 2015
Accepted	19 OCT 2015
Accepted article online	18 NOV 2015

Supporting information
available online



Keywords: Astaxanthin · Biosynthesis · Complete genome · Discrete distribution · *Sphingomonas*

1 Introduction

Astaxanthin (3,3'-dihydroxy- β -carotene-4,4'-dione) belongs to a large class of phytochemicals known as terpenes. Studies have shown that astaxanthin has beneficial effects on human health, including cancer prevention, immune response enhancement, cardiovascular disease prevention, radiation resistance, and biological antioxidant protection [1]. Recently, astaxanthin has been used in many applications, such as nutritional supplements, pharmaceuticals, cosmetics, food colorants, and animal feed additives [2–6], and the worldwide market of astaxanthin is expected to increase dramatically.

Currently, astaxanthin is obtained by chemical synthesis or solvent-based extraction from natural sources, such as the green alga *Haematococcus pluvialis* [7] and the yeast *Xanthophyllomyces dendrorhous* (formerly known as *Phaffia rhodozyma*) [8]. A few studies have also

Correspondence: Prof. Tiangang Liu, Key Laboratory of Combinatorial Biosynthesis and Drug Discovery (Wuhan University), Ministry of Education, Wuhan University School of Pharmaceutical Sciences, Donghu Road, 430071 Wuhan, PR China
E-mail: liutg@whu.edu.cn

Abbreviations: **CrtB**, phytoene synthase; **CrtE**, geranylgeranyl pyrophosphate synthase; **CrtI**, phytoene dehydrogenase; **CrtY**, lycopene cyclase; **CrtZ**, β -carotene hydroxylase; **CrtW**, β -carotene ketolase; **DMAPP**, dimethylallyl pyrophosphate; **EGFP**, enhanced green fluorescent protein; **FPP**, farnesyl pyrophosphate; **gDNA**, genomic DNA; **GGPP**, geranylgeranyl diphosphate; **Idi**, isopentenyl-diphosphate delta-isomerase; **IPP**, isopentenyl pyrophosphate; **MEP**, 2-C-Methyl-D-erythritol 4-phosphate; **MVA**, mevalonate; **PBcR**, PacBio corrected read; **SMRT**, single-molecule, real-time

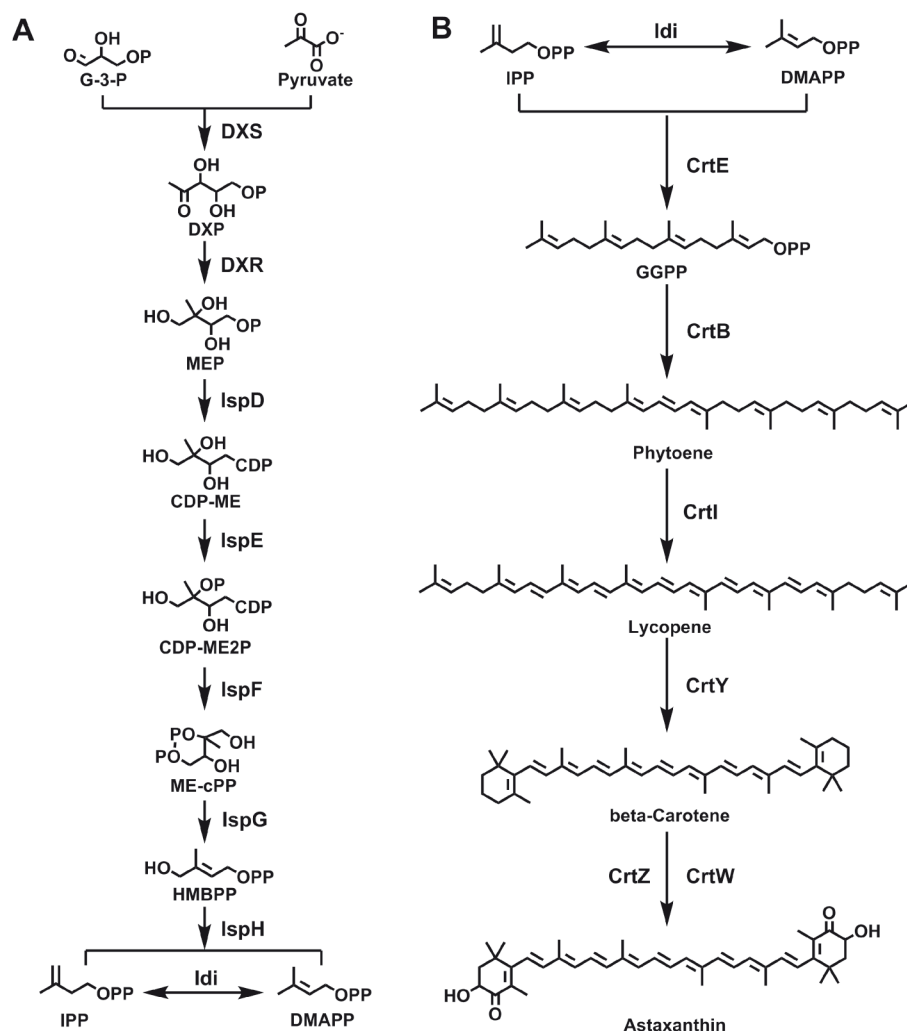


Figure 1. Proposed astaxanthin biosynthetic pathway in *Spingomonas* sp. ATCC 55669. (A) In the strain *Spingomonas* sp. ATCC 55669, upstream events via the MEP pathway to get the precursors IPP and DMAPP. (B) The downstream carotenoid pathway involved the conversion of intermediates IPP and DMAPP to astaxanthin. DXS, 1-deoxy-D-xylulose-5-phosphate synthase; DXR, 1-deoxy-D-xylulose-5-phosphate reductoisomerase; IspD, 2-C-methyl-D-erythritol 4-phosphate cytidyltransferase; IspE, 4-diphosphocytidyl-2-C-methyl-D-erythritol kinase; IspF, 2-C-methyl-D-erythritol 2,4-cyclodiphosphate synthase; IspG, (E)-4-hydroxy-3-methylbut-2-enyl-diphosphate synthase; IspH, 4-hydroxy-3-methylbut-2-enyl diphosphate reductase. G-3-P, D-glyceraldehyde 3-phosphate; DXP, 1-deoxy-D-xylulose 5-phosphate; CDP-ME, 4-(cytidine 5'-diphospho)-2-C-methyl-D-erythritol; CDP-ME2P, 2-phospho-4-(cytidine 5'-diphospho)-2-C-methyl-D-erythritol; ME-cPP, 2-C-methyl-D-erythritol 2,4-cyclodiphosphate; HMBPP, 1-hydroxy-2-methyl-2-butenyl 4-diphosphate.

evaluated astaxanthin production in bacteria such as *Paracoccus* [9] and *Brevundimonas* genera [10]. However, astaxanthin production is limited by low yields and limited natural sources. Therefore, researchers have focused on discovering novel microbial producers of astaxanthin to meet the growing demand for astaxanthin.

In biological systems, astaxanthin contains a C_{40} methyl-branched hydrocarbon backbone derived from successive condensation of eight C_5 isoprene units. The C_5 isoprene unit IPP, can be generated from an acetyl-CoA precursor via the MVA pathway [11] or from pyruvate and glyceraldehyde-3-phosphate precursors via the MEP pathway [12]. In these two pathways, the extended unit IPP is isomerized to DMAPP by IPP isomerase, which is encoded by the *idi* gene. DMAPP is then condensed with the extended unit IPP to form astaxanthin. Six proteins participate in this condensation process: CrtE, CrtB, CrtI, CrtY, CrtW, and CrtZ (Fig. 1).

Spingomonas spp. are strictly aerobic, rod-shaped, chemoheterotrophic gram-negative bacteria that harbor glycosphingolipids, rather than lipopolysaccharides, in

their cell membranes, which distinguishes them from traditional gram-negative bacteria. *Spingomonas* is widely distributed in many different aquatic and terrestrial habitats [13], and has been shown to be able to survive in low-nutrient conditions and metabolize a broad range of organic compounds, including refractory environmental pollutants [14–16]. In addition, some *Spingomonas* can produce useful high value-added products, such as carotenoids [17].

Whole-genome sequencing has been widely applied to decode the functional activities of microbes, and a complete, highly accurate genome sequence is a critical starting point for mining the genetic features. High-throughput sequencing technologies play an important role in obtaining such genome sequences [18]. Specifically, third-generation sequencing (TGS) PacBio SMRT technology provides an improved microbial genome assembly method with extended read lengths and a lack of GC bias. The majority of errors during PacBio sequencing occur because of random indels [19], which can be mostly corrected by SMRT dozens-fold coverage sequencing reads. However, a small number of indel

errors can persist in PacBio-assembled genomes, limiting the accuracy of gene prediction. In contrast, Illumina sequencing, a traditional next-generation sequencing technology (TNGS), generates highly accurate short-length reads with very few indel errors but with many gaps during de novo genome assembly [20, 21]. Hybrid error correction takes advantage of the strengths of both sequencing approaches.

In this study, we identified and characterized the astaxanthin-producing ability of strain *Sphingomonas* sp. ATCC 55669 by complete genome sequencing using a combined PacBio-Illumina approach and gene annotation. Our results described this new astaxanthin producer and provided important insights into astaxanthin biosynthesis in *Sphingomonas*, revealing novel biosynthesis components for bioengineering.

2 Materials and methods

2.1 Strains, media, and reagents

The strain *Sphingomonas* sp. ATCC 55669 was cultured in #272 nutrient glucose medium (8.0 g dehydrated nutri-

ent broth [Difco-BD, Corpus Christi, TX, USA] with 5.0 g glucose/L distilled H₂O) at 26.0°C in the dark with shaking (220 rpm). *E. coli* K-12 MG1655 (DE3) was cultured in Luria broth (LB; containing 10.0 g/L NaCl, 10.0 g/L tryptone, and 5.0 g/L yeast extract) at 30.0°C in the dark with shaking (220 rpm). *E. coli* XL1-Blue was used to replicate plasmids and construct clones. All media were autoclaved at 115°C for 30 min. The strains used in this study are listed in Table 1. The astaxanthin standard was purchased from Aladdin (Seattle, WA, USA).

2.2 Preparation of genomic DNA of *Sphingomonas* sp. ATCC 55669 for genome sequencing

Sphingomonas sp. ATCC 55669 was cultured overnight. 50 mL of the culture was collected and centrifuged for 5 min at 5000 rpm. The pellet was resuspended in 10 mL distilled water and SET buffer (75 mM NaCl, 25 mM EDTA, 20 mM Tris-Cl), centrifuged again, and resuspended with 5 mL SET buffer. Next, 450 µL of lysozyme (100 mg/mL) was added, and the cell suspension was incubated in a 37°C water bath for 2 h. 10 µL of RNase A (10 mg/mL) was added, followed by incubation for additional 20 min. Proteinase K (300 µL, 20 mg/mL) was added,

Table 1. Strains and plasmids used in this study.

Strain	Description	Source
<i>Sphingomonas</i> sp. ATCC 55669	Isolated from Quebec Canada	American Type Culture Collection
<i>E. coli</i> K-12 MG1655 (DE3)	F ⁺ λ: ilvG- rfb-50 rph-1 (DE3)	Prof. Kristala Prather from MIT
A1	<i>E. coli</i> K-12 MG1655 (DE3): pMH1, pFZ81, pFZ153	This study
A2	<i>E. coli</i> K-12 MG1655 (DE3): pMH1, pFZ81, pTM3518	This study
A3	<i>E. coli</i> K-12 MG1655 (DE3): pMH1, pFZ81, pTM2108	This study
A4	<i>E. coli</i> K-12 MG1655 (DE3): pMH1, pFZ81, pTM0906	This study
A5	<i>E. coli</i> K-12 MG1655 (DE3): pMH1, pFZ81, pTM2930	This study
A6	<i>E. coli</i> K-12 MG1655 (DE3): pMH1, pFZ81, pTM1181	This study

Plasmid	Backbone	Relevant genotype	Source
pMH42	pET28a(+)	pT7: N-terminal His-tagged EGFP, Kan ⁺	This study
pTMB2E	pBBR1MCS-2	plac: EGFP, Kan ⁺	This study
pTMB2I	pBBR1MCS-2	plac: Idi, Kan ⁺	This study
pGZI	pET28a(+)	pT7: N-terminal His-tagged Idi, Kan ⁺	[26]
pFZ87	pETDuet-1	pT7: Idi, Amp ⁺	This study
pFZ152	pETDuet-1	pT7: CrtY, CrtZ, CrtW, Amp ⁺	This study
pFZ21	pET28a(+)	pT7: N-terminal His-tagged CrtE, Kan ⁺	[31]
pFZ22	pET28a(+)	pT7: N-terminal His-tagged CrtB, Kan ⁺	[31]
pFZ23	pET28a(+)	pT7: N-terminal His-tagged CrtI, Kan ⁺	[31]
pFZ112	pETDuet-1	pT7: CrtE, CrtI, CrtB, Amp ⁺	This study
pFZ153	pETDuet-1	pT7: CrtE, CrtI, CrtB, pT7: Idi, CrtY, CrtZ, CrtW, Amp ⁺	This study
pTM3518	pETDuet-1	pT7: CrtE _{sp1} , CrtI, CrtB, pT7: Idi, CrtY, CrtZ, CrtW, Amp ⁺	This study
pTM2108	pETDuet-1	pT7: CrtE _{sp2} , CrtI, CrtB, pT7: Idi, CrtY, CrtZ, CrtW, Amp ⁺	This study
pTM0906	pETDuet-1	pT7: CrtE _{sp3} , CrtI, CrtB, pT7: Idi, CrtY, CrtZ, CrtW, Amp ⁺	This study
pTM2930	pETDuet-1	pT7: CrtE, CrtI, CrtB, pT7: Idi, CrtY, CrtZ _{sp1} , CrtW, Amp ⁺	This study
pTM1181	pETDuet-1	pT7: CrtE, CrtI, CrtB, pT7: Idi, CrtY, CrtZ _{sp2} , CrtW, Amp ⁺	This study
pMH1	pBBR1MCS-1	plac: AtoB, ERG13 and N-terminal His-tagged tHMG1, Cam ⁺	[26]
pFZ81	pBBR1MCS-2	plac: ERG12, ERG8, MVD1 and N-terminal His-tagged Idi, Kan ⁺	[26]

and samples were incubated at 37°C in a water bath for 40 min. Finally, 5 mL of 10% SDS was added, followed by incubation at 55°C for 2 h. 2 mL of 5 M NaCl was added, and samples were mixed gently. The DNA mixture was then transferred to a round-bottomed centrifuge tube, and 10 mL chloroform was added. After thorough, gentle mixing, samples were centrifuged at 12 000 rpm for 10 min. The upper aqueous phase was collected, and 10 mL chloroform was added; the mixing and centrifugation steps were repeated twice. DNA was then precipitated with 0.7 volumes of isopropanol and spooled into a 1.5-mL centrifuge tube with a glass rod. Finally, DNA was washed with 1 mL of cold 70% ethanol for 1 min, dried, and redissolved in at least 200 µL nuclease-free water at room temperature.

2.3 Genome sequencing, genome assembly, and gene prediction

Both Illumina and PacBio SMRT sequencing technology were used to obtain the genome of strain *Sphingomonas* sp. ATCC 55669. For Illumina sequencing, gDNA was fragmented to an average size of 350 bp without pre-PCR amplification, and HiSeq2000 was used for sequencing. For PacBio reads, gDNA was fragmented to an average size of 10 kb, and genome sequencing was performed by PacBio RS with 8 SMRT cells in a 90-min sequencing reaction. An additional SMRT library was built with gDNA fragmented to an average size of 900 bp. Sequencing of this library was performed by PacBio RS with 14 SMRT cells in two 45-min sequencing reactions.

Both strategies of PacBio-only consensus calling and hybrid error correction with Illumina reads were performed for PacBio long reads, and BLASR [22] alignment was used with an error rate of 0.25 and minimum overlap length of 40 bp. A SMRT 900 bp library was constructed to help correct PacBio long reads, and final PBcRs were obtained from all SMRT 900 bp library data. Genome assembly was carried out with Celera Assembler [23], and the longest 25-fold PBcR data were assembled with an utgErrorRate set to 0.05 and minimum overlap length of 40 bp. Genome indel detection was performed with the Burrows-Wheeler transform algorithm based on short-read alignment. The SOAPaligner [24] was used with a required identity of more than 95% for Illumina paired-read alignment. The continuous gap size was limited to 3 bp. Reads Alignment Showing Tools software (RAS-Tools: <https://sourceforge.net/projects/rastools>) was used for alignment with match-level and gap flag functions for consensus sequences.

Whole-genome gene predictions were performed using the interpolated Markov model [25]. Long ORFs were scanned by GLIMMER 3.0 [25] to generate the training set. Start codon usage was then analyzed with the Estimated Locations of Pattern Hits software from

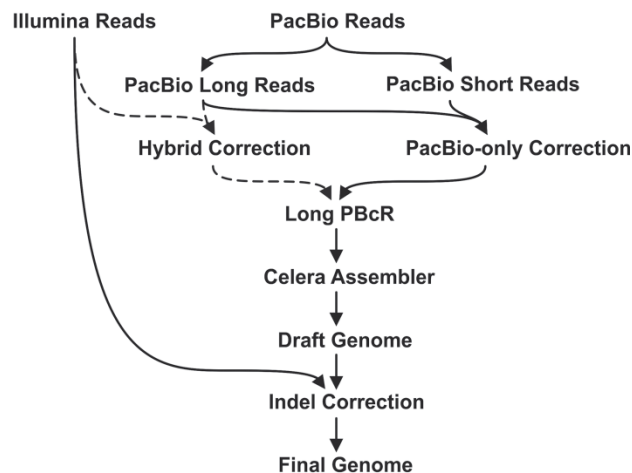


Figure 2. Assembly strategy used in this study. Shorter PacBio reads were used to correct indel errors of longer PacBio reads and followed by contig assembly. Illumina reads were used to correct persistent indel errors in contigs.

<http://cbcb.umd.edu/software/ELPH/>. Genetic table 11 was used for gene prediction.

Figure 2 summarizes the steps taken to integrate Illumina and PacBio SMRT sequencing technology in this study.

2.4 Plasmid construction for astaxanthin functional gene identification

The plasmids used in this study are listed in Table 1, and the primers used are listed in Supporting information, Table S1. The *idi* gene from *E. coli*, obtained from pGZI [26], was cloned into the plasmid pETDuet-1 digested with *Nde*I and *Xho*I to yield pFZ87. The *crtY* and *crtZ* genes were amplified individually from *Pantoea agglomerans* [27, 28] with primers *Idi-PagCrtY-F/CrtZ-PagCrtY-R* and *CrtY-PagCrtZ-F/CrtW-PagCrtZ-R*. The *crtW* gene from *Brevundimonas* sp. SD212 [29], codon-optimized and synthesized by Genescript (Torrens Park, South Australia), was amplified with primers *CrtZ-BreCrtW-F* and *BreCrtW-R*. The four fragments containing genes *idi*, *crtY*, *crtZ*, and *crtW* were assembled to yield plasmid pFZ152 via the Gibson method [30]. The *crtE*, *crtI*, and *crtB* genes were separately amplified from pFZ21, pFZ22, and pFZ23 [31] with primers *Duet-PanCrtE-F/PanCrtI-CrtE-R*, *PanCrtE-CrtI-F/PanCrtB-CrtI-R*, and *PanCrtI-CrtB-F/Duet-EcoRI-PanCrtB-R*, respectively. Then, these three fragments with genes *crtE*, *crtI*, and *crtB* were assembled via the Gibson method to yield plasmid pFZ112. Finally, the fragment from pFZ112 including genes *crtE*, *crtI*, and *crtB* was digested with *Nde*I-*Eco*RI and inserted into pFZ152 to yield plasmid pFZ153. Plasmid pFZ153, which contained *crtEIB-idi-crtYZW*, served as a positive control to confer astaxanthin production ability in *E. coli*.

For identifying genes involved in astaxanthin biosynthesis from *Sphingomonas* sp. ATCC 55669, the homologous gene in plasmid pFZ153 was replaced. Specifically, *crtE*_{Sp1} (gene locus_tag in NCBI: *MC45_16265*), *crtE*_{Sp2} (gene locus_tag in NCBI: *MC45_09750*), and *crtE*_{Sp3} (gene locus_tag in NCBI: *MC45_04155*) were amplified from the *Sphingomonas* sp. ATCC 55669 genome with primers Duet-Pan3518-F2/PanCrtI-3518-R, Duet-Pan2108-F2/PanCrtI-2108-R, and Duet-Pan0906-F2/PanCrtI-0906-R, respectively. The three fragments replaced *crtE* in plasmid pFZ153 to obtain pTM3518, pTM2108, and pTM0906. *crtZ*_{Sp1} (gene locus_tag in NCBI: *MC45_13565*) and *crtZ*_{Sp2} (gene locus_tag in NCBI: *MC45_05470*) were amplified with primers CrtY-Pag2930-F/CrtW-Pag2930-R and CrtY-Pag1181-F2/CrtW-Pag1181-R. The two fragments replaced *crtZ* in pFZ153 to obtain pTM2930 and pTM1181.

2.5 Overexpression of exogenous genes in *Sphingomonas* sp. ATCC 55669

The gene encoding EGFP was amplified from a commercial plasmid using primers EGFP-A and EGFP-S; the fragment was inserted into pET28a(+) digested with *Nde*I and *Eco*RI to yield pMH42 and then re-amplified with primers EGFP-pBBR-S and EGFP-pBBR-A using pMH42 as a template. The amplified fragment was inserted into pBBR1MCS2 digested with *Kpn*I and *Sac*I to yield pTMB2E. EGFP expression was controlled by the IPTG-inducible *lacZ* promoter. To transfer pTMB2E to *Sphingomonas* sp. ATCC 55669, electrocompetent *Sphingomonas* sp. ATCC 55669 cells were prepared. Cells were grown to an OD₆₀₀ of 0.2–0.4, collected on ice, washed with ice-cold 10% glycerol, and collected again by centrifugation. Cells were then washed with ice-cold 10% glycerol, kept on ice for 30 min, and pelleted by centrifugation. After washing with 10% glycerol, cells were resuspended with 0.04 volumes of ice-cold 10% glycerol. For each reaction, 120 µL of cells was mixed with 2 µL (about 100 ng) of pTMB2E. Cells were then transferred to a 2-mm precooled electroporation cuvette, electroporated at 3 kV for 4.5–5 ms, and recovered with 800 µL of #272 medium. Recovered cells were incubated with shaking for 2 h at 26°C, spread on #272 agar plates supplemented with 60 mg/L kanamycin, and cultured at 26°C for at least three days. The resulting clones were picked up and cultured in #272 broth with 60 mg/L kanamycin. When OD₆₀₀ of the cultures reached 0.6–0.8, IPTG was added to a final concentration of 0.1 mM. After 24 h of cultivation, fluorescence microscopy was used to detect EGFP expression. *Sphingomonas* sp. ATCC 55669 with pBBR1MCS2 served as the negative control.

The target IPP isomerase gene *idi* was derived from plasmid pGZI [26]. The gene was amplified using primers *idi*-pET28a-A and *idi*-pET28a-S and inserted into pBBR1MCS2 digested with *Bam*HI and *Sac*I to yield

pTMB2I. With the above-mentioned electrotransformation method, pTMB2I was transformed into *Sphingomonas* sp. ATCC 55669.

2.6 Astaxanthin identification

To detect astaxanthin from *Sphingomonas* sp. ATCC 55669, the pellet was collected by centrifugation and extracted with 1:4 (v:v) methanol and acetone by vortexing in the dark until residues were colorless. The supernatant was dried and redissolved in acetone, centrifuged, and transferred to sample vials for LC-MS detection. The LC-MS system (LTQ Orbitrap XL [Thermo Scientific, Waltham, MA, USA]) was equipped with a DIONEX Acclaim 120 C18 (4.6 mm × 250 mm × 5 µm) column. The chromatographic conditions were as follows: 95% buffer A (H₂O with 0.1% formic acid) and 5% buffer B (acetonitrile with 0.1% formic acid) at 1 mL/min for 2 min; buffer A was decreased to 50% over 13 min and then to 5% over 25 min; maintained at 95% B and 5% A for 15 min; buffer A was increased to 95% over 1 min and maintained until 60 min. MS was carried out using the full scan method to detect the parent ion (597.394).

2.7 Shake-flask fermentation and quantification of astaxanthin produced by *Sphingomonas* sp. ATCC 55669

Sphingomonas sp. ATCC 55669 and the mutant carrying recombinant pTMB2I or pBBR1MCS2 were cultured in #272 medium at 26.0°C in the dark with shaking (220 rpm). When OD₆₀₀ of the cultures reached 0.6–0.8, IPTG was added to a final concentration of 0.1 mM. After 60 h, cells were collected for product detection. Astaxanthin was extracted and quantified using LC-MS (Triple Stage Quadrupole Quantum [Thermo Scientific]) with a Thermo Hypersil Gold C18 (2.1 mm × 100 mm × 5 µm) column. The mobile phases and gradient used were as follows: isocratic 50% buffer A (H₂O with 0.1% formic acid) and 50% buffer B (acetonitrile with 0.1% formic acid) at 0.35 mL/min for 2 min; buffer A was decreased to 2% over 8 min and maintained for 8 min; buffer A was increased to 50% over 0.1 min and maintained until 20 min. MS was then carried out using the multiple reaction monitoring (MRM) transition [32] to detect the parent ion (597.394) and product ion (147.200).

2.8 Shake-flask fermentation and quantification of astaxanthin produced by *E. coli*

During *E. coli* K-12 MG1655 (DE3) shake-flask fermentation, the *E. coli* strain carrying pMH1 and pFZ81, which overexpressed upstream MVA pathway components provided adequate precursors of IPP and DMAPP [26].

Mutants A1–A6, carrying pMH1, pFZ81 and pFZ153, pTM3518, pTM2108, pTM0906, pTM2930, or pTM1181,

were cultured in 500-mL flasks with 200 mL LB supplemented with 34 mg/L chloramphenicol, 50 mg/L kanamycin, and 100 mg/L ampicillin. The flasks were incubated at 30°C with shaking (200 rpm). When OD₆₀₀ reached 0.7–0.9, IPTG was added to a final concentration of 0.1 mM. 8 h later, 2 mL of each culture was harvested, and astaxanthin was extracted as described above. The Dionex UltiMate 3000 HPLC system (Thermo Scientific) equipped with a Dionex Acclaim 120 C18 (4.6 mm × 250 mm × 5 μm) column was used for astaxanthin quantification. Samples were separated with mobile phases A (H₂O with 0.1% trifluoroacetic acid) and B (acetonitrile with 0.1% trifluoroacetic acid) at a flow rate of 1.0 mL/min. The column temperature was 25°C, and detection occurred at 478 nm. Mobile phase compositions varied as follows: 0 min, 50% B; 5 min, 100% B; 20 min, 100% B; 25 min, 50% B; 27 min, 50% B.

3 Results

3.1 Confirmation of astaxanthin production in *Sphingomonas* sp. ATCC 55669

The product isolated from *Sphingomonas* sp. ATCC 55669 cells cultured in #272 nutrient glucose medium was analyzed by LC-MS, and a molecule at *m/z* (597.392) was obtained at the same retention time as the astaxanthin standard (Supporting information, Fig. S1), suggesting that this strain naturally produced astaxanthin. Quantitative analysis indicated that *Sphingomonas* sp. ATCC 55669 produced 1.2 μg/g cdw (cells dry weight) astaxanthin. *Sphingomonas astaxanthinifaciens* was the first astaxanthin-producing bacterium identified in this genus [33], and thus, we explored *Sphingomonas* sp. ATCC 55669 as another host for astaxanthin production.

3.2 Combined PacBio-Illumina sequencing strategy for the complete genome of *Sphingomonas* sp. ATCC 55669

The SMRT 10 kbp library was sequenced with PacBio RS, yielding 393 Mbp raw reads (read N50 length: 4028 bp; mean read quality: 0.856). After removal of the adapter sequence, 378 Mbp reads remained (N50 length: 3220 bp; Supporting information, Fig. S2). A SMRT 900 bp library was built to generate more reads to correct the PacBio long reads, and 1.69 Gbp raw reads were achieved by PacBio RS (N50 length: 3824 bp; mean quality: 0.862). After removal of the adapter sequence, 1.3 Gbp reads remained (N50 length: 450 bp).

Both 100-fold coverage Illumina reads and SMRT 900 bp PacBio reads were used to correct SMRT 10 kbp long reads. With 100-fold coverage from Illumina sequence data, hybrid error correction resulted in 300 Mbp PBcRs (N50 length: 1402 bp), whereas 100-fold coverage from

PacBio data yielded 327 Mbp PBcRs (N50 length: 2647 bp). Thus, the two strategies yielded similar data size, but the hybrid error correction strategy generated half the N50 length (Supporting information, Fig. S3). Final PBcRs were corrected with all data from the SMRT 900 bp library, yielding 327 Mbp reads (N50 length: 2756 bp).

Genome assembly was performed with PacBio-only corrected PBcRs, and three contigs remained with a total size of 4.07 Mbp and an N90 length greater than 3.86 Mbp. Using SOAPaligner, more than 96.85% of Illumina reads aligned to these three contigs with over 95% identity. Each contig showed more than 4 kbp self-repeat of two edges by dot plot analysis, and PCR verification revealed that the self-repeat was false; the contigs represented a single copy of the circular genome. Further genome coverage analysis of the Illumina reads showed that the poorly covered genomic area was less than 1000 bp. Forty-eight single nucleotide insertions were detected with RASTools, and each insertion had at least 14 supported Illumina reads. Twenty-three low-coverage regions were verified by Sanger sequencing, and the results indicated that the low coverage in these regions may be explained by the randomly distributed Illumina short read sequencing strategy, whereas some indel errors may persist with the PacBio-only assembly. With gene prediction, most of insertion sites after correction showed higher similarity with the existing reference sequences (Supporting information, Fig. S4). The final genome contained a 3.86-Mbp circular chromosome and two circular plasmids with 163 and 39 kbp, respectively, at a GC content of 68.48% (Fig. 3; GenBank CP009571-CP009573).

3.3 Bioinformatics analysis and engineering of astaxanthin biosynthetic pathway of *Sphingomonas* sp. ATCC 55669 by expressing an exogenous *idi* gene

From the complete genome sequence, 4023 putative ORFs were identified. All the predicted genes involved in astaxanthin biosynthesis could be found uniquely and with high homology. The homology of the predicted genes with annotations in the NCBI nr database is listed in Supporting information, Table S2. The upstream biosynthetic pathway belonged to the MEP pathway, and the downstream astaxanthin biosynthetic pathway was the same as that found in most bacteria. Among the predicted genes, *ispDF₅* had the highest homology with strain *Sphingomonas wittichii* RW1, which had both 2-*C*-methyl-D-erythritol 4-phosphate cytidylyltransferase and 2-*C*-methyl-D-erythritol 2,4-cyclodiphosphate synthase domains. In addition, all genes related to astaxanthin biosynthesis were unique, except *idi*, *crtE*, and *crtZ*.

The *idi* gene, which encodes a key enzyme in the isoprenoid pathway, was absent from this system. In order to exploit the astaxanthin-producing strain *Sphingomonas*

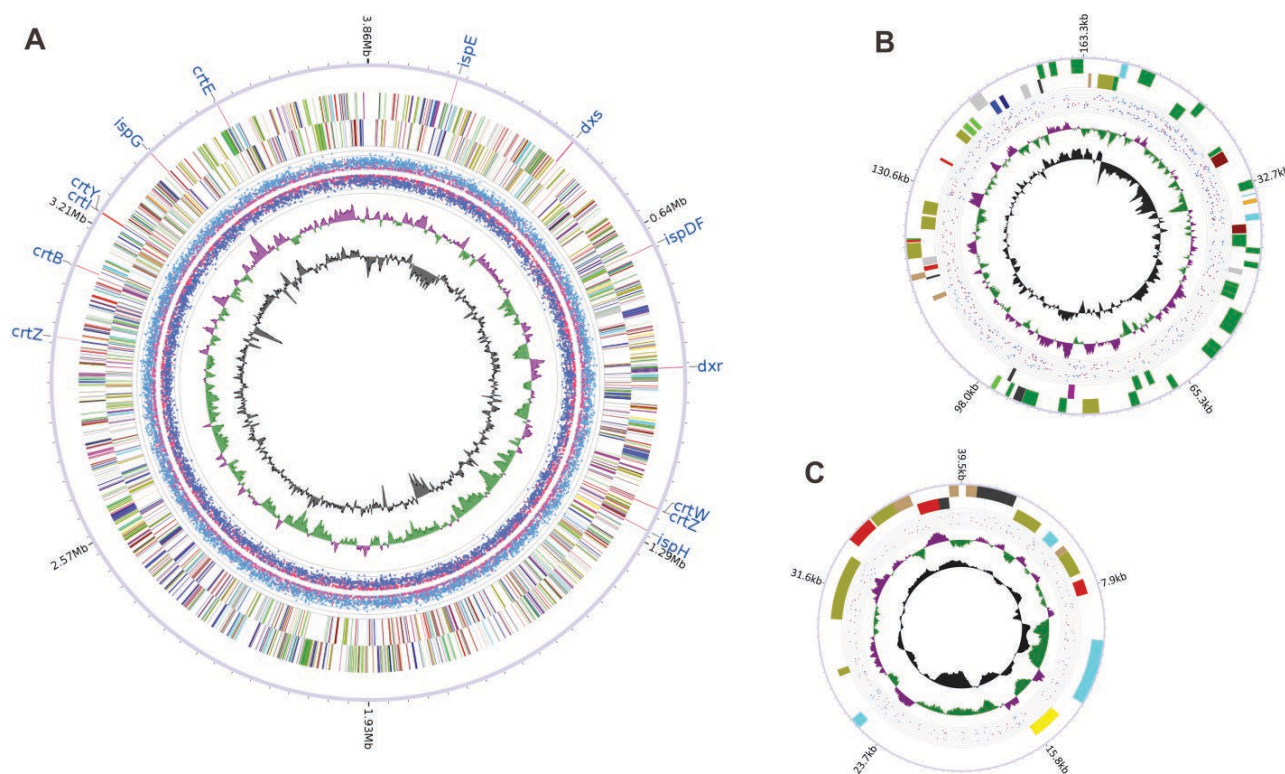


Figure 3. The complete genome of *Sphingomonas* sp. ATCC 55669 contained three circular DNAs: one chromosome (A) and two megaplasmsids (B, C). From innermost to outermost circles: GC content; GC-skew $([G - C] / [G + C])$; methylation information of forward sequences (red, m4C; blue, 6mA); methylation information of reverse sequences (pink, m4C; cyan, 6mA); predicted genes color-coded by COG categories of forward and reverse strands, respectively; and genes related to the non-mevalonate pathway and carotenoid biosynthesis. All genes putatively involved in astaxanthin biosynthesis (gene names noted in the outer circle) showed a discrete distribution throughout the chromosome.

sp. ATCC 55669, we attempted to establish a genetic manuscript method. Detection of EGFP as a reporter for gene expression indicated that the exogenous gene could be transformed into this strain and expressed with the pBBR1MCS ori and promoter P_{lac} (Supporting information, Fig. S5A and S5B). Overexpression of exogenous *idi* in *Sphingomonas* sp. ATCC 55669 caused a 5.4-fold increase in astaxanthin production compared to the strain without exogenous *idi* (Supporting information, Fig. S5C). The mutant harboring pTMB2I produced 6.91 $\mu\text{g/g}$ cdw astaxanthin, whereas that harboring pBBR1MCS2 only produced 1.29 $\mu\text{g/g}$ cdw.

Two *crtZ* candidates (*crtZ*_{Sp1} and *crtZ*_{Sp2}) were homologous to strains *Pantoea ananatis* and *Paracoccus* sp. N81106 at about 60% identity. For *crtE*, no candidates with at least 30% identity were found. Candidates with between 20 and 30% identity were compared in terms of catalytic function domains. Finally, three *crtE* candidates (*crtE*_{Sp1}, *crtE*_{Sp2}, and *crtE*_{Sp3}) were chosen (Supporting information, Table S2). These candidates all catalyzed IPP condensation into the substrate. In the carotenoid biosynthetic pathway, FPP synthase, with high homology to *crtE*_{Sp1}, could catalyze the condensation of IPP and DMAPP to FPP, a precursor for GGPP synthesis. In addition, octaprenyl

diphosphate synthase, with high homology to *crtE*_{Sp2}, and isoprenyl transferase, with high homology to *crtE*_{Sp3}, could also catalyze the formation of FPP from IPP.

3.4 Heterologous overproduction for critical genes involved in the astaxanthin biosynthesis of *Sphingomonas* sp. ATCC 55669 in *E. coli*

In order to identify the predicted function of genes involved in astaxanthin biosynthesis, a carotenoid synthesis platform was constructed in *E. coli*. According to bioinformatic analysis of astaxanthin biosynthetic genes, two *crtZ* candidates (*crtZ*_{Sp1} and *crtZ*_{Sp2}) and three *crtE* candidates (*crtE*_{Sp1}, *crtE*_{Sp2}, and *crtE*_{Sp3}) were identified. The result indicated that only one candidate (*crtE*_{Sp1}) had *crtE* function, whereas both *crtZ*_{Sp1} and *crtZ*_{Sp2} had *crtZ* function. Importantly, the nonfunctional *crt* genes in the system did not have corresponding roles, illustrating that the functional genes carried out the catalytic functions of the known genes in the proposed pathway. With the high-efficiency targeted engineering carotenoid synthesis platform, four astaxanthin-producing strains, i.e. A1, A2, A5, and A6 (harboring pFZ153, pTM3518, pTM2930, and pTM1181, respectively) produce 6.6, 4.44, 1.12, and

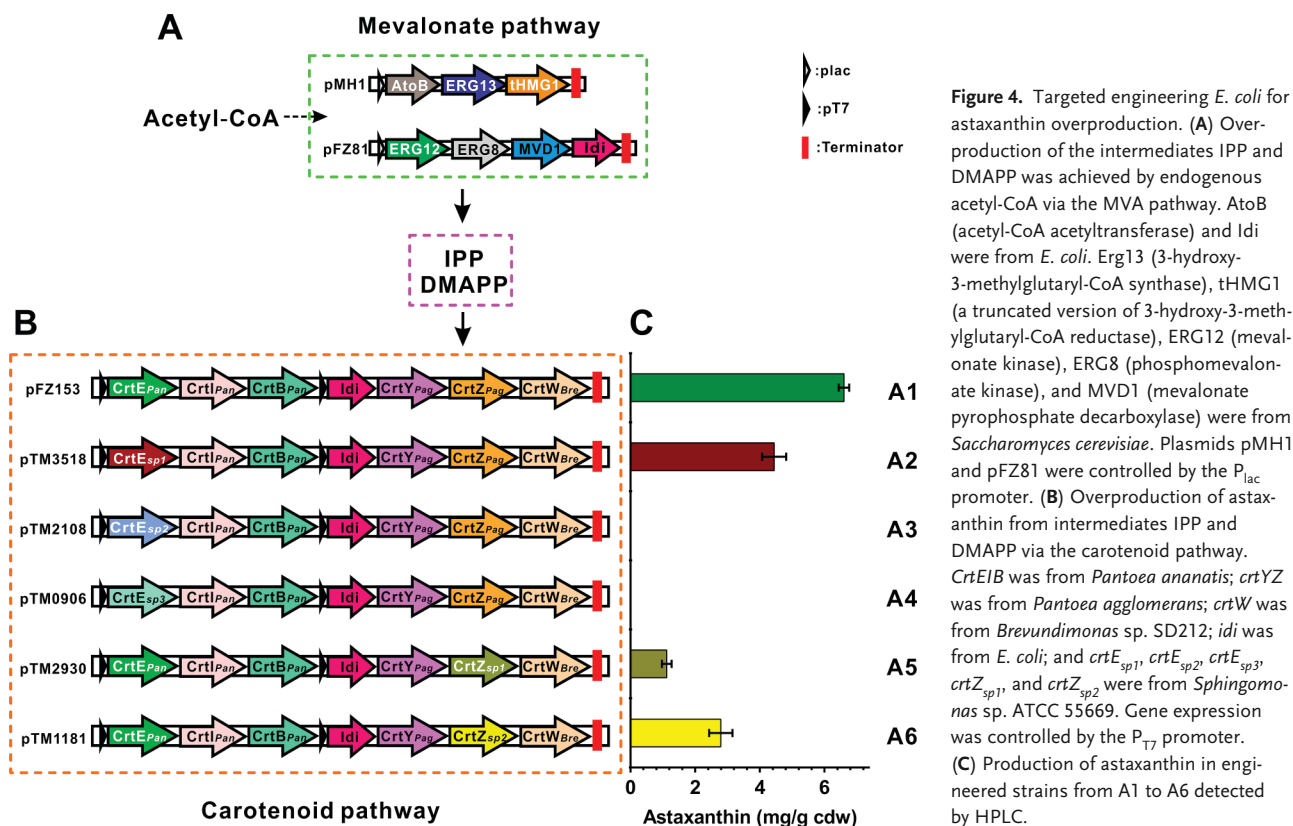


Figure 4. Targeted engineering *E. coli* for astaxanthin overproduction. (A) Overproduction of the intermediates IPP and DMAPP was achieved by endogenous acetyl-CoA via the MVA pathway. AtoB (acetyl-CoA acetyltransferase) and Idi were from *E. coli*. Erg13 (3-hydroxy-3-methylglutaryl-CoA synthase), tHMG1 (a truncated version of 3-hydroxy-3-methylglutaryl-CoA reductase), ERG12 (mevalonate kinase), ERG8 (phosphomevalonate kinase), and MVD1 (mevalonate pyrophosphate decarboxylase) were from *Saccharomyces cerevisiae*. Plasmids pMH1 and pFZ81 were controlled by the P_{lac} promoter. (B) Overproduction of astaxanthin from intermediates IPP and DMAPP via the carotenoid pathway. *CrtEIB* was from *Pantoea ananatis*; *crtYZ* was from *Pantoea agglomerans*; *crtW* was from *Brevundimonas* sp. SD212; *idi* was from *E. coli*; and *crtE_{sp1}*, *crtE_{sp2}*, *crtE_{sp3}*, *crtZ_{sp1}*, and *crtZ_{sp2}* were from *Sphingomonas* sp. ATCC 55669. Gene expression was controlled by the P_{T7} promoter. (C) Production of astaxanthin in engineered strains from A1 to A6 detected by HPLC.

2.79 mg/g cdw astaxanthin, respectively, at 8 h after induction (Fig. 4).

From this analysis, we clarified the entire astaxanthin biosynthesis pathway and found that the genes involved in astaxanthin biosynthesis were distributed throughout the chromosome of *Sphingomonas* sp. ATCC 55669 (Fig. 3).

4 Discussion

In this study, we found that *Sphingomonas* sp. ATCC 55669 naturally produced astaxanthin. Astaxanthin is beneficial to human health, enhancing immune system function and providing protection against lipid-membrane oxidation and DNA damage. The demand for natural astaxanthin is expected to grow rapidly, with an annual worldwide market estimated at US\$200 million [34]. However, natural bioresources of astaxanthin are limited. Therefore, exploration of novel resources for production of natural astaxanthin may help meet this demand.

4.1 A combined PacBio-Illumina approach for highly accurate complete genome sequence of *Sphingomonas* sp. ATCC 55669

A combined PacBio-Illumina approach, which provides an error correction for the draft genome produced by PacBio

with Illumina reads, generated a complete, highly accurate genome sequence. Illumina sequencing technology contains the least indel error and has multi-fold coverage, Indel errors could be cut down to zero, as could base substitutions, yielding accurate result for many comparison purposes. However, there were still many gaps, preventing detailed analysis. PacBio sequencing technology produced long reads, but with 15.4–17.9% randomly distributed indel errors [35, 36]. Most error correction strategies have used TNGS technologies to produce high-accuracy reads to correct SMRT long reads [19]. However, optimized traditional sequence alignment strategies are generally used to detect substitution errors. The interference of indel errors created inconsistencies between PacBio long and short reads. We used BLASR to align indel-rich PacBio long reads, and PBcR accuracy significantly increased, allowing overlap extension after error correction. RAS-Tools reduced the indel errors of PacBio long reads, but we preferred to use error correction for the draft genome produced by PacBio with Illumina reads. This sequencing technology combination and assembly method allowed us to obtain the complete genome sequence.

4.2 Astaxanthin biosynthetic genes and genes distribution of *Sphingomonas* sp. ATCC 55669

All genes involved in astaxanthin biosynthesis of *Sphingomonas* sp. ATCC 55669 were described herein. In the

carotenoid biosynthetic pathway, the MEP pathway is upstream of the precursors IPP and DMAPP for astaxanthin production. Bacteria harboring the MEP pathway have been shown to lack the *idi* gene [37]. In carotenoid biosynthesis, *idi*, which balances IPP and DMAPP levels, has been shown to control carbon flow into downstream pathways [26]. However, *idi* was absent in *Sphingomonas* sp. ATCC 55669. Interestingly, overexpression of *idi* in this strain increased astaxanthin production by nearly 5.4-fold, supporting the important role of *idi* on carotenoid production in *Sphingomonas* sp. ATCC 55669. With the functional identification platform in *E. coli*, *crtE_{Sp1}*, *crtZ_{Sp1}*, and *crtZ_{Sp2}* were shown to have corresponding functions in astaxanthin biosynthesis. *CrtE_{Sp1}* had about 43% protein identity with FPP synthase, which catalyzes IPP and DMAPP to form FPP; FPP then absorbs IPP to generate GGPP. In this case, we found that *crtE_{Sp1}* functioned to condense IPP and DMAPP to GGPP. *CrtZ_{Sp1}* and *crtZ_{Sp2}* had low specificity, consistent with a previous study [38]. Thus, this first study of the astaxanthin biosynthetic pathway in *Sphingomonas* revealed additional astaxanthin biosynthetic components for bioengineering.

Astaxanthin biosynthetic genes were distributed throughout the chromosome in *Sphingomonas* sp. ATCC 55669. In general, most genes involved in natural product production exist in the form of gene clusters, as has been described for astaxanthin production [39]. However, the genome of *Sphingomonas* sp. ATCC 55669 was unique, with discrete distribution of the genes.

4.3 Production of astaxanthin in engineered *E. coli* and engineered *Sphingomonas* sp. ATCC 55669

In our targeted engineering carotenoid system constructed in *E. coli*, we produced up to 6.6 mg/g cdw astaxanthin, which was lower than the yield reported for the engineered microbe *Xanthophyllomyces dendrorhous* (up to 9 mg/g cdw) [40], but higher than the production in *E. coli* (2 mg/g cdw) [41]. Thus, this targeted engineering method effectively increased astaxanthin production; we were even able to achieve production of 8.64 mg/g cdw astaxanthin in the A1 mutant at 4 h after induction.

In order to express exogenous genes in *Sphingomonas* sp. ATCC 55669, a genetic manipulation method was successfully established using a simple method that shared some elements, such as plasmids and promoters, with *E. coli*. This may facilitate future attempts at genetic engineering in this genus. Indeed, *Sphingomonas* has recently attracted attention in the field of environmental microbiology as a potential metabolizer for a broad range of organic compounds, particularly refractory environmental pollutants, and for production of useful exopolysaccharides and carotenoids. Thus, this genetic method could be not only used in degradative engineering but also for carotenoid overproduction.

In conclusion, we demonstrated that *Sphingomonas* sp. ATCC 55669 naturally produced astaxanthin. The complete genome was sequenced using PacBio-Illumina sequencing. Subsequently, the entire astaxanthin biosynthetic pathway, including some new astaxanthin biosynthesis components, was identified. Genes were discretely distributed throughout the chromosome. We believe this work provides important insights into the identification of natural product biosynthetic pathways based on sequencing technology, particularly for cases in which genes are discretely distributed or even absent. Moreover, our study described an additional genetic source for astaxanthin production.

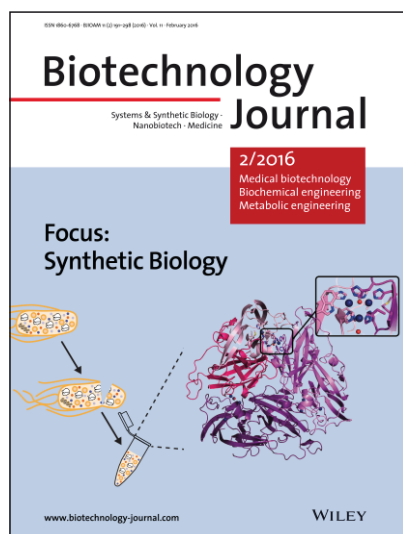
We would like to thank Pacific Biosciences and Geroge Yuan for PacBio sequencing and assembly. This work was supported by the Ministry of Science and Technology of China 973 Grants (2012CB721000 and 2011CBA00800) and 863 Grants (2012AA02A701), the National Natural Science Foundation of China (31222002), the Science and Technology Department of Hubei Province and Doctoral Fund of Ministry of Education of China (20110141120028).

The authors declare no financial or commercial conflict of interest.

5 References

- [1] Higuera-Ciapara, I., Felix-Valenzuela, L., Goycoolea, F. M., Astaxanthin: A review of its chemistry and applications. *Crit. Rev. Food Sci.* 2006, 46, 185–196.
- [2] Fraser, P. D., Bramley, P. M., The biosynthesis and nutritional uses of carotenoids. *Prog. Lipid Res.* 2004, 43, 228–265.
- [3] Borowitzka, M., Micro-algae as sources of fine chemicals. *Curr. Microbiol.* 1986, 3, 372–375.
- [4] Tominaga, K.; Hongo, N.; Karato, M.; Yamashita, E, Cosmetic benefits of astaxanthin on humans subjects. *Acta Biochim. Pol.* 2012, 59, 43–47.
- [5] Dufosse L, Microbial production of food grade pigments. *Food Technol. Biotechnol.* 2006, 44, 313–21.
- [6] Breithaupt, D., Modern application of xanthophylls in animal feeding – a review. *Trends Food Sci. Technol.* 2007, 18, 501–506.
- [7] Bubrick, P., Production of astaxanthin from *Haematococcus*. *Biore-sour. Technol.* 1991, 38, 237–239.
- [8] Miller, M., Yoneyama, M., Soneda, M., *Phaffia*, a new yeast genus in the *Deuteromycotina* (*Blastomycetes*). *Int. J. Syst. Bacteriol.* 1976, 26, 286–291.
- [9] Yokoyama, A., Izumida, H., Miki, W., Production of astaxanthin and 4-ketoastaxanthin by the marine bacterium, *Agrobacterium aurantiacum*. *Biosci. Biotechnol. Biochem.* 1994, 58, 1842–1844.
- [10] Yokoyama, A., Miki, W., Izumida, H., Shizuri, Y., New trihydroxy-keto-carotenoids isolated from an astaxanthin-producing marine bacterium. *Biosci. Biotechnol. Biochem.* 1996, 60, 200–203.
- [11] Bloch, K., Chaykin, S., Phillips, A. H., de Waard, A., Mevalonic acid pyrophosphate and isopentenylpyrophosphate. *J. Biol. Chem.* 1959, 234, 2595–2604.

- [12] Rohmer, M., Knani, M., Simonin, P., Sutter, B., Sahn, H., Isoprenoid biosynthesis in bacteria: A novel pathway for the early steps leading to isopentenyl diphosphate. *Biochem. J.* 1993, *295*, 517–524.
- [13] Takeuchi, M., Hamana, K., Hiraishi, A., Proposal of the genus *Sphingomonas sensu stricto* and three new genera, *Sphingobium*, *Novosphingobium* and *Sphingopyxis*, on the basis of phylogenetic and chemotaxonomic analyses. *Int. J. Syst. Evol. Microbiol.* 2001, *51*, 1405–1417.
- [14] Fang, H. H., Liang, D., Zhang, T., Aerobic degradation of diethyl phthalate by *Sphingomonas* sp. *Bioresour. Technol.* 2007, *98*, 717–720.
- [15] Shokrollahzadeh, S., Azizmohseni, F., Golmohammad, F., Shokouhi, H., Khademhaghighat, F., Biodegradation potential and bacterial diversity of a petrochemical wastewater treatment plant in Iran. *Bioresour. Technol.* 2008, *99*, 6127–6133.
- [16] Zhong, Y., Luan, T., Lin, L., Liu, H., Tam, N. F., Production of metabolites in the biodegradation of phenanthrene, fluoranthene and pyrene by the mixed culture of *Mycobacterium* sp. and *Sphingomonas* sp. *Bioresour. Technol.* 2011, *102*, 2965–2972.
- [17] Silva, C., Cabral, J., Van Keulen, F., Isolation of a β -carotene overproducing soil bacterium, *Sphingomonas* sp. *Biotechnol. Lett.* 2004, *26*, 257–262.
- [18] Didelot, X., Bowden, R., Wilson, D. J., Peto, T. E., Crook, D. W., Transforming clinical microbiology with bacterial genome sequencing. *Nat. Rev. Genet.* 2012, *13*, 601–612.
- [19] Koren, S., Schatz, M. C., Walenz, B. P., Martin, J. et al., Hybrid error correction and de novo assembly of single-molecule sequencing reads. *Nat. Biotechnol.* 2012, *30*, 693–700.
- [20] Jünemann, S., Sedlazeck, F. J., Prior, K., Albersmeier, A. et al., Updating benchtop sequencing performance comparison. *Nat. Biotechnol.* 2013, *31*, 294–296.
- [21] Loman, N. J., Misra, R. V., Dallman, T. J., Constantinidou, C. et al., Performance comparison of benchtop high-throughput sequencing platforms. *Nat. Biotechnol.* 2012, *30*, 434–439.
- [22] Chaisson, M. J., Tesler, G., Mapping single molecule sequencing reads using basic local alignment with successive refinement (BLASR): Application and theory. *BMC Bioinf.* 2012, *13*, 238.
- [23] Miller, J. R., Delcher, A. L., Koren, S., Venter, E. et al., Aggressive assembly of pyrosequencing reads with mates. *Bioinformatics* 2008, *24*, 2818–2824.
- [24] Li, R., Yu, C., Li, Y., Lam, T.-W. et al., SOAP2: An improved ultrafast tool for short read alignment. *Bioinformatics* 2009, *25*, 1966–1967.
- [25] Delcher, A. L., Bratke, K. A., Powers, E. C., Salzberg, S. L., Identifying bacterial genes and endosymbiont DNA with Glimmer. *Bioinformatics* 2007, *23*, 673–679.
- [26] Zhu, F., Zhong, X., Hu, M., Lu, L. et al., In vitro reconstitution of mevalonate pathway and targeted engineering of farnesene overproduction in *Escherichia coli*. *Biotechnol. Bioeng.* 2014, *111*, 1396–1405.
- [27] Hundle, B., Alberti, M., Nievelstein, V., Beyer, P. et al., Functional assignment of *Erwinia herbicola* Eho10 carotenoid genes expressed in *Escherichia coli*. *Mol. Gen. Genet.* 1994, *245*, 406–416.
- [28] Schnurr, G., Schmidt, A., Sandmann, G., Mapping of a carotenogenic gene cluster from *Erwinia herbicola* and functional identification of six genes. *FEMS Microbiol. Lett.* 1991, *78*, 157–161.
- [29] Nishida, Y., Adachi, K., Kasai, H., Shizuri, Y. et al., Elucidation of a carotenoid biosynthesis gene cluster encoding a novel enzyme, 2,2'- β -hydroxylase, from *Brevundimonas* sp. strain SD212 and combinatorial biosynthesis of new or rare xanthophylls. *Appl. Environ. Microbiol.* 2005, *71*, 4286–4296.
- [30] Gibson, D. G., Enzymatic assembly of overlapping DNA fragments. *Method Enzymol.* 2011, *498*, 349–361.
- [31] Zhu, F., Lu, L., Fu, S., Zhong, X. et al., Targeted engineering and scale up of lycopene overproduction in *Escherichia coli*. *Process Biochem.* 2014, *50*, 341–346.
- [32] Anderson, L., Hunter, C. L., Quantitative mass spectrometric multiple reaction monitoring assays for major plasma proteins. *Mol. Cell. Proteomics* 2006, *5*, 573–588.
- [33] Asker, D., Beppu, T., Ueda, K., *Sphingomonas astaxanthinifaciens* sp. nov., a novel astaxanthin-producing bacterium of the family *Sphingomonadaceae* isolated from Misasa, Tottori, Japan. *FEMS Microbiol. Lett.* 2007, *273*, 140–148.
- [34] Lorenz, R. T., Cysewski, G. R., Commercial potential for *Haematococcus* microalgae as a natural source of astaxanthin. *Trends Biotechnol.* 2000, *18*, 160–167.
- [35] Chin, C. S., Sorenson, J., Harris, J. B., Robins, W. P. et al., The origin of the Haitian cholera outbreak strain. *New Engl. J. Med.* 2011, *364*, 33–42.
- [36] Rasko, D. A., Webster, D. R., Sahl, J. W., Bashir, A. et al., Origins of the *E. coli* strain causing an outbreak of hemolytic-uremic syndrome in Germany. *New Engl. J. Med.* 2011, *365*, 709–717.
- [37] Jordi, P.-G., Manuel, R.-C., Metabolic plasticity for isoprenoid biosynthesis in bacteria. *Biochem. J.* 2013, *452*, 19–25.
- [38] Choi, S.-K., Matsuda, S., Hoshino, T., Peng, X., Misawa, N., Characterization of bacterial β -carotene 3,3'-hydroxylases, CrtZ, and P450 in astaxanthin biosynthetic pathway and adonirubin production by gene combination in *Escherichia coli*. *Appl. Microbiol. Biotechnol.* 2006, *72*, 1238–1246.
- [39] Sedkova, N., Tao, L., Rouvière, P. E., Cheng, Q., Diversity of carotenoid synthesis gene clusters from environmental *Enterobacteriaceae* strains. *Appl. Environ. Microbiol.* 2005, *71*, 8141–8146.
- [40] Gassel, S., Breitenbach, J., Sandmann, G., Genetic engineering of the complete carotenoid pathway towards enhanced astaxanthin formation in *Xanthophyllomyces dendrorhous* starting from a high-yield mutant. *Appl. Microbiol. Biotechnol.* 2014, *98*, 345–350.
- [41] Scaife, M. A., Burja, A. M., Wright, P. C., Characterization of cyanobacterial β -carotene ketolase and hydroxylase genes in *Escherichia coli*, and their application for astaxanthin biosynthesis. *Biotechnol. Bioeng.* 2009, *103*, 944–955.



Biotechnology Journal – list of articles published in the February 2016 issue.

Editorial

Transforming biotechnology with synthetic biology

George Guo-Qiang Chen and Michael C. Jewett

<http://dx.doi.org/10.1002/biot.201600010>

BTJ-Forum

In Memoriam of Prof. Bernard Witholt

Manfred Zinn, Sang Yup Lee and George Guo-Qiang Chen

<http://dx.doi.org/10.1002/biot.201500096>

BTJ-Forum

Meeting Report:

Cold Spring Harbor Asia Synthetic Biology Meeting

Ivan Hajnal

<http://dx.doi.org/10.1002/biot.201400836>

Review

Minimal genome:

Worthwhile or worthless efforts toward being smaller?

Donghui Choe, Suhyung Cho, Sun Chang Kim and Byung-Kwan Cho

<http://dx.doi.org/10.1002/biot.201400838>

Research Article

Cell-free protein synthesis enables high yielding synthesis of an active multicopper oxidase

Jian Li, Thomas J. Lawton, Jan S. Kostecki, Alex Nisthal, Jia Fang, Stephen L. Mayo, Amy C. Rosenzweig and Michael C. Jewett

<http://dx.doi.org/10.1002/biot.201500030>

Research Article

Engineering of core promoter regions enables the construction of constitutive and inducible promoters in *Halomonas* sp.

Tingting Li, Teng Li, Weiyue Ji, Qiuyue Wang, Haoqian Zhang, Guo-Qiang Chen, Chunbo Lou and Qi Ouyang

<http://dx.doi.org/10.1002/biot.201400828>

Research Article

Genome mining of astaxanthin biosynthetic genes from *Sphingomonas* sp. ATCC 55669 for heterologous overproduction in *Escherichia coli*

Tian Ma, Yuanjie Zhou, Xiaowei Li, Fayin Zhu, Yongbo Cheng, Yi Liu, Zixin Deng and Tiangang Liu

<http://dx.doi.org/10.1002/biot.201400827>

Research Article

A cell-free expression and purification process for rapid production of protein biologics

Challise J. Sullivan, Erik D. Pendleton, Henri H. Sasmor, William L. Hicks, John B. Farnum, Machiko Muto, Eric M. Amendt, Jennifer A. Schoborg, Rey W. Martin, Lauren G. Clark, Mark J. Anderson, Alaksh Choudhury, Raffaella Fior, Yu-Hwa Lo, Richard H. Griffey, Stephen A. Chappell, Michael C. Jewett, Vincent P. Mauro and John Dresios

<http://dx.doi.org/10.1002/biot.201500214>

Research Article

Co-production of hydrogen and ethanol from glucose by modification of glycolytic pathways in *Escherichia coli* – from Embden-Meyerhof-Parnas pathway to pentose phosphate pathway

Eunhee Seol, Balaji Sundara Sekar, Subramanian Mohan Raj and Sunghoon Park

<http://dx.doi.org/10.1002/biot.201400829>

Research Article

A fluorescein-labeled AmpC β -lactamase allows rapid characterization of β -lactamase inhibitors by real-time fluorescence monitoring of the β -lactamase-inhibitor interactions

Man-Wah Tsang, Pak-Ho Chan, Sze-Yan Liu, Kwok-Yin Wong and Yun-Chung Leung

<http://dx.doi.org/10.1002/biot.201400861>

Research Article

Alphavirus capsid proteins self-assemble into core-like particles in insect cells: A promising platform for nanoparticle vaccine development

Mia C. Hikke, Corinne Geertsema, Vincen Wu, Stefan W. Metz, Jan W. van Lent, Just M. Vlak and Gorben P. Pijlman

<http://dx.doi.org/10.1002/biot.201500147>

Research Article

Cell-free protein synthesis of a cytotoxic cancer therapeutic: Onconase production and a just-add-water cell-free system

Amin S. M. Salehi, Mark Thomas Smith, Anthony M. Bennett, Jacob B. Williams, William G. Pitt and Bradley C. Bundy

<http://dx.doi.org/10.1002/biot.201500237>

Research Article

Non-monotonic course of protein solubility in aqueous polymer-salt solutions can be modeled using the sol-mxDLVO model

Marcel Herhut, Christoph Brandenbusch and Gabriele Sadowski

<http://dx.doi.org/10.1002/biot.201500123>

Biotech Method

Rational plasmid design and bioprocess optimization to enhance recombinant adeno-associated virus (AAV) productivity in mammalian cells

Verena V. Emmerling, Antje Pegel, Ernest G. Milian, Alina Venereo-Sanchez, Marion Kunz, Jessica Wegele, Amine A. Kamen, Stefan Kochanek and Markus Hoerer

<http://dx.doi.org/10.1002/biot.201500176>